

Phellodendronoside A Exerts Anticancer Effects Depending on Inducing Apoptosis Through ROS/Nrf2/Notch Pathway and Modulating Metabolite Profiles in Hepatocellular Carcinoma

Yanpo Si^{1,2}, Chengcheng Hui¹, Tao Guo^{1,2}, Mengqi Liu¹, Xiaohui Chen³, Chunhong Dong^{3,4}, Shuying Feng⁵

¹Department of Pharmacy, Henan University of Chinese Medicine, Zhengzhou, People's Republic of China; ²Henan Engineering Research Center of Medicinal and Edible Chinese Medicine, Zhengzhou, People's Republic of China; ³Academy of Chinese Medical Sciences, Henan University of Chinese Medicine, Zhengzhou, People's Republic of China; ⁴Henan Key Laboratory of Chinese Medicine for Polysaccharides and Drugs Research, Zhengzhou, People's Republic of China; ⁵Medical College, Henan University of Chinese Medicine, Zhengzhou, People's Republic of China

Correspondence: Tao Guo; Shuying Feng, Henan University of Chinese Medicine, No. 156 JinshuiEast Road, Zhengzhou, 450046, People's Republic of China, Tel +86 371 65962746; +86 371 65934070, Email gt010010@hactcm.edu.cn; fsy@hactcm.edu.cn

Purpose: To reveal the potential mechanism of PDA on hepatocellular carcinoma SMMC-7721 cells in vitro.

Methods: The cytotoxic activity, colony formation, cell cycle distribution, apoptosis and their associated protein analysis, intracellular reactive oxygen species (ROS) and Ca²⁺ levels, proteins in Nrf2 and Ntoch pathways and metabolite profiles of PDA against hepatocellular carcinoma were investigated.

Results: PDA with cytotoxic activity inhibited cell proliferation and migration, increased intracellular ROS, Ca²⁺ levels and MCUR1 protein expression in a dose-dependent manner, caused cell cycle arrest in the S phase and induced apoptosis via adjusting the levels of Bcl-2, Bax, and Caspase 3 proteins, and inhibited the activation of Notch1, Jagged, Hes1, Nrf2 and HO-1 proteins. Metabonomics data showed that PDA significantly regulated 144 metabolite levels tend to be normal level, especially carnitine derivatives, bile acid metabolites associated with hepatocellular carcinoma, and mainly enriched in ABC transporter, arginine and proline metabolism, primary bile acid biosynthesis, Notch signaling pathway, etc, and proved that PDA markedly adjusted Notch signaling pathway.

Conclusion: PDA exhibited the proliferation inhibition of SMMC-7721 cells by inhibiting ROS/Nrf2/Notch signaling pathway and significantly affected the metabolic profile, suggesting PDA could be a potential therapeutic agent for patients with hepatocellular carcinoma.

Keywords: isoquinoline alkaloid, apoptosis, acylcarnitine, bile acids, metabolomics

Introduction

Hepatocellular carcinoma (HCC), as the third cancer killer after lung cancer and colorectal cancer, is one of the commonest primary liver malignancies threatening the health of people worldwide.^{1,2} According to the latest survey data, the number of new cases of HCC worldwide was 91 million, and the number of deaths was 83 million in 2020.³ Its higher morbidity and mortality are mainly related to its characteristics of asymptomatic, rapid growth and high aggressiveness, for this reason, clinically, most patients are usually diagnosed as locally advanced or metastatic or inoperable due to complications.⁴ Study has shown that the main factors that trigger HCC include chronic with hepatitis B or C virus infection, aflatoxin-contaminated foodstuffs, chronic alcohol consumption, etc, in most cases, cirrhosis is the strongest risk factor for HCC.⁵

Current drugs used clinically to treat HCC remain a concern for patients due to their drug resistance and side effects.⁶ Therefore, the search for new drugs to treat HCC has become a focus of global researchers. In recent years, natural medicine, especially traditional Chinese medicines with clear curative effects, has possessed a significant guiding role in the development of new drugs, a large number of natural products have been proven to play an important role in the prevention and treatment of

various diseases, including cancer, Alzheimer's disease, hypertension and insomnia.⁷⁻⁹ *Phellodendron chinense* Schneid (Rutaceae), as a traditional medicinal plant, has been used widely to quench the fire and clear heat, dry dampness and counteract toxicity in the field of traditional Chinese medicine for centuries.¹⁰ More recently, researchers from various countries have studied the chemical composition and biological activity of *P. chinense*, showing that alkaloids are its main components, especially isoquinoline alkaloids.¹¹ Pharmacological studies have confirmed that alkaloids have a variety of pharmacological activities, including anti-inflammatory, immune-enhancing, hypolipidemic, hypoglycemic, and antitumor effects.¹² Notably, berberine, the active alkaloid ingredient in *P. chinense*, has shown significant inhibitory effects against various cancers, such as lung cancer, liver cancer, colorectal cancer, ovarian cancer and prostate cancer.¹³ Isoquinoline alkaloids derivatives, as a class of *N*-heterocyclic active ingredients widely present in the plant, have a high probability of success as lead compounds in the drug discovery and development process,¹⁴ which was reflected in several isoquinoline alkaloid-based drugs, such as the antirheumatic sinomenine, the antitussive codeine, the analgesic morphine, and the acetylcholinesterase inhibitor galanthamine.¹⁵ Thus, novel isoquinoline alkaloids from natural products as promising drug leads remain an active area of drug development.

In our previous work, the isoquinoline alkaloids derivative, Phellodendronoside A (PDA) was isolated from the bark of *P. chinense* in our lab, which possessed potent anti-inflammatory activity against lipopolysaccharide-induced RAW264.7 cells¹⁰ and anticancer activity, while being less toxic to normal hepatocyte lines. So, we expected that PDA, as an isoquinoline alkaloid, could be a new drug for the treatment of cancer, just like berberine. In this research, the anticancer mechanism of PDA had been elucidated by molecular biological methods including MTT, colony formation assay, flow cytometry and Western blot. The global metabolic profiling of SMMC7721 cells induced by PDA was investigated using a non-targeted metabolomics approach based on ultra-performance liquid chromatography-mass spectrometry/mass spectrometry (UPLC-MS/MS).

Materials and Methods

Instruments, Reagents, and Antibodies

Ultra-High-Performance Liquid Chromatography (Dionex, USA); High-speed refrigerated centrifuge (Eppendorf, Germany); GAPDH (GB15002), Caspase3 (GB11009-1), Hes1 (GB11374), CyclinD1 (GB111935), CyclinE1 (GB111938), BCL-2 (GB113375), Jagged (GB11122), Notch1 (GB111690), horseradish peroxidase (HRP) conjugated goat anti-mouse (GB25301) and goat anti-rabbit (GB23303), and Bax (GB12690) were purchased from Wuhan servicebio Technology CO., LTD. MCUR1 (13706, CST), HO-1 (25614-1-AP) and Nrf2 (16396-1-ap) were ordered from Proteintech, Wuhan.

Cell Culture

Human HCC cell lines, SMMC-7721, provided by Prof. Suiqing Chen (Henan University of Chinese Medicine, China), were cultured using RPMI 1640 medium (20210823, Solarbio, Beijing, China) containing 10% fetal bovine serum (FBS, 04-001-1ACS, BI, Israel), 100 U/mL penicillin and 100 µg/mL streptomycin (Solarbio, China) at 37°C in a humidified carbon dioxide incubator with 5% CO₂. SMMC-7721 cell lines were authenticated using short tandem repeat DNA testing by the FuHeng Center in March 2022. All studies were approved by the Ethics Committee of the Henan University of Chinese Medicine and conducted in accordance with its guidelines.

Cytotoxic Assay

MTT assay was used to determine the cytotoxicity of PDA on SMMC-7721 cells. SMMC-7721 cells (3×10^3 cells/well) were seeded in a 96-well plate for 24 h, and PDA with purity greater than 98% was diluted with 1640 into different concentrations (25, 30, 35, 40, 45, 50 µmol/L) and treated for 24 h. Then, 20 µL of Thiazolyl Blue Tetrazolium Bromide (MTT, M8180, Solarbio, Beijing, China) solution was added and incubated at 37°C for another 4 h. 150 µL of DMSO was added to the wells where the MTT solution was removed. Finally, the absorbance of the solution was measured at 490 nm.

Colony Formation Assay

The colony formation assay was used to assess the inhibitory effect of PDA on cell proliferation. Cells were inoculated at 1×10^3 cells/well in 6-well plates and cultured for 2 weeks until the colonies were formed, and the medium was changed every 3 days with fresh medium. Afterwards, the colonies were fixed with 70% ethanol and stained with crystal violet, and then the wells were washed to image and count the colonies.

Cell Cycle Distribution Analysis

Flow cytometry (FCM) was used to evaluate the effect of PDA on the cell cycle distribution of SMMC-7721. Cells (1.5×10^5 cells/well) were collected after PDA treatment for 24 h and fixed overnight in 70% ethanol. Cells were centrifuged, washed and incubated with RNase A solution (200 $\mu\text{g/mL}$). Afterwards, PI solution (100 $\mu\text{g/mL}$) was added and incubated again in darkness. Cells were detected by FCM (FACSCalibur, BD, USA).

Apoptosis Analysis

FCM was used to detect intracellular apoptosis levels. Cells in 6-well plates (1.5×10^5 cells/well) were incubated with PDA for 24 h and suspended in a binding buffer. Subsequently, 5 μL of Annexin V-FITC and 5 μL of PI (556547, BD, USA) were added into the buffer, respectively, and flow analysis was performed immediately after incubation in the dark.

Intracellular ROS Analysis

Cellular ROS levels were measured using the Reactive Oxygen Assay Kit (Beyotime). Briefly, cells that had been incubated with PDA for 24 h were collected in 6-well plates (1.5×10^5 cells/well). The DCFH-DA probe was added to the cells and incubated for 20 min at 37°C . Subsequently, cells were washed three times with PBS and DCF fluorescence was measured by FCM.

Determination of Intracellular Ca^{2+}

A Ca^{2+} detection assay kit (20171206, Solarbio Science & Technology, Beijing China) was used to evaluate the level of cellular Ca^{2+} . SMMC-7721 cells were inoculated into 6-well plates at 1.5×10^5 per well. After 24 h of culture, the cells were collected and incubated with 500 μL Fluo-4 (AM) for 20 min; then, five times the volume of HBSS containing 1% fetal bovine serum was added and cultured for 40 min. The cells were washed with HEPES buffer and detected by FCM.

Western Blot

Cells were collected from 6-well plates (5×10^4 cells/mL, 3 mL) after 24 h incubation with PDA and lysed on ice with RIPA lysis buffer. Protein concentration in the supernatant was quantified using the BCA Protein Assay Kit (G2026, Servicebio, Wuhan, China). Equal amounts of protein samples (40 μg) were separated by sodium dodecyl sulfate-polyacrylamide gel electrophoresis (SDS-PAGE) and electrically transferred to polyvinylidene difluoride (PVDF) membranes. The membranes were blocked with 0.1% Tween-20 (TBST) containing 5% skimmed dry milk powder for 4 h and incubated with primary antibody (dilution 1:1000) in a shaking incubator at 4°C overnight, washed with TBST and then incubated with enzyme-labeled secondary antibody (dilution 1:500) blocking solution for 1 h. Finally, the target proteins were detected using BosterECL Star Western blotting detection reagent (AR1170, BOSTER, Wuhan, China).

UPLC-MS/MS Analysis

The UPLC-MS/MS analysis was performed as described technique in a previous article by our team.⁹ Briefly, the cell supernatant obtained by homogenization was analyzed via a UPLC-ESI-MS/MS data acquisition instrument system (MS, QTRAP® System, UPLC, Shim-pack UFLC SHIMADZU CBM30A system): Waters ACQUITY UPLC HSS T3 C18 (1.8 μm , 2.1 mm \times 100 mm); mobile phase A as ultrapure water with 0.04% acetic acid and mobile phase B was acetonitrile with 0.04% acetic acid; elution gradient. LIT and triple quadrupole scans were gained on a triple quadrupole-linear ion trap mass spectrometer (QTRAP), QTRAP® LC-MS/MS System.

Statistical Analysis

Data from at least 3 independent experiments were expressed as means \pm standard deviation (SD). Statistical analysis of variance in multiple group comparisons was performed using one-way analysis of variance (ANOVA) and followed by SNK post-hoc for group-wise comparisons in Statistical Product and Service Solutions (SPSS) 25.0 software. $P < 0.05$ was considered statistically different. Raw data obtained by UPLC-MS/MS were processed by Pro-file Analysis software and subjected to principal component analysis (PCA) and orthogonal partial least squares discriminant analysis (OPLS-DA) to obtain score plots. Potential markers (p -value < 0.05 and VIP value > 1.0) were screened using the Human Metabolome Database (HMDB), METLIN and other databases. Identified molecules were entered into the Kyoto Encyclopedia of Genes and Genomes (KEGG) for metabolic pathway analysis.

Results

PDA Inhibits Cell Proliferation and Colony Formation

The chemical structure of PDA is shown in [Figure 1A](#). Cell viability was assessed by treatment with PDA at 0, 25, 30, 35, 40, 45 and 50 μM for 24 h. As shown in [Figure 1B](#), PDA displayed significant cytotoxicity at 30 $\mu\text{mol/L}$ compared with the control group and inhibited the proliferation of SMMC-7721 cells in a dose-dependent manner. PDA treatment at concentrations of 25, 30, 35, 40, 45 and 50 μM exhibits 6.88%, 18.08%, 29.20%, 41.42%, 48.06% and 49.47% of inhibition on cell viability, respectively, and the IC_{50} value of PDA was $\sim 47.52 \mu\text{mol/L}$. Thus, PDA at concentrations of 30–40 $\mu\text{mol/L}$ was selected for further studies.

Afterward, the long-term cytotoxicity of PDA to SMMC-7721 cells was detected by cell colony formation. As shown in [Figure 1C](#) and [D](#), chronic exposure to PDA (30–40 $\mu\text{mol/L}$) also dose-dependently inhibited colony formation and decreased the numbers of SMMC-7721 cell colonies.

PDA Causes Cell Cycle Arrest in the S Phase

As shown in [Figure 2A](#) and [B](#), PDA treatment for 24 h resulted in cell cycle arrest in the S phase in a dose-dependent manner. As the concentration of PDA increased, the proportion of S phase cells on SMMC-7721 cells increased from 26.8% (0 μM) to 49.9% (40 μM), while the proportion of G0/G1 phase cells decreased from 49.8% (0 μM) to 27.2% (40 μM), with no significant effect on the proportion of G2/M-phase cells. Afterward, cyclins were also detected ([Figure 2C–E](#)), the expression of cyclin E was down-regulated, while cyclin D1 was up-regulated after PDA intervention, which was consistent with the cell cycle results detected by flow cytometry.

PDA Induces Apoptosis

The results showed that the apoptosis rates of SMMC-7721 cells (the sum of early and late apoptosis) increased from 0.08% (0 μM) to 22.35% (40 μM) ([Figure 3A](#) and [B](#)), indicating that PDA induced apoptosis in a dose-dependent manner. In addition, the expressions of apoptosis-related proteins were further examined ([Figure 3C](#)). The quantitative results showed that PDA could significantly decrease the expression of Bcl-2 protein, increase the expression of Bax, and ultimately activate Caspase 3 to induce apoptosis in SMMC-7721 cells ([Figure 3D–F](#)).

PDA Inhibits Cell Proliferation by Inhibiting ROS/Nrf2/Notch Pathway

ROS, a by-product of the oxidative phosphorylation process, can also inhibit proliferation in cancer cells by promoting apoptosis.¹⁶ Intracellular ROS and Ca^{2+} levels increased in a dose-dependent manner after treatment with 30–40 μM PDA for 24 h compared with the control group ([Figure 4A](#) and [B](#)). Besides, after 24 h of treatment with PDA, the expressions of Notch1, Jagged, Hes1, MCUR1, Nrf2, and HO-1 were detected, which were thought to be associated with abnormally elevated ROS in the cells. As shown in [Figure 4C](#) and [D](#), the results indicated that PDA also dose-dependently increased the expression of cellular MCUR1 protein and decreased the expression of Notch1, Jagged, Hes1, Nrf2 and HO-1 proteins ([Figure 4E–I](#)), indicating that PDA inhibited cell proliferation by inhibiting ROS/Nrf2/Notch pathway.

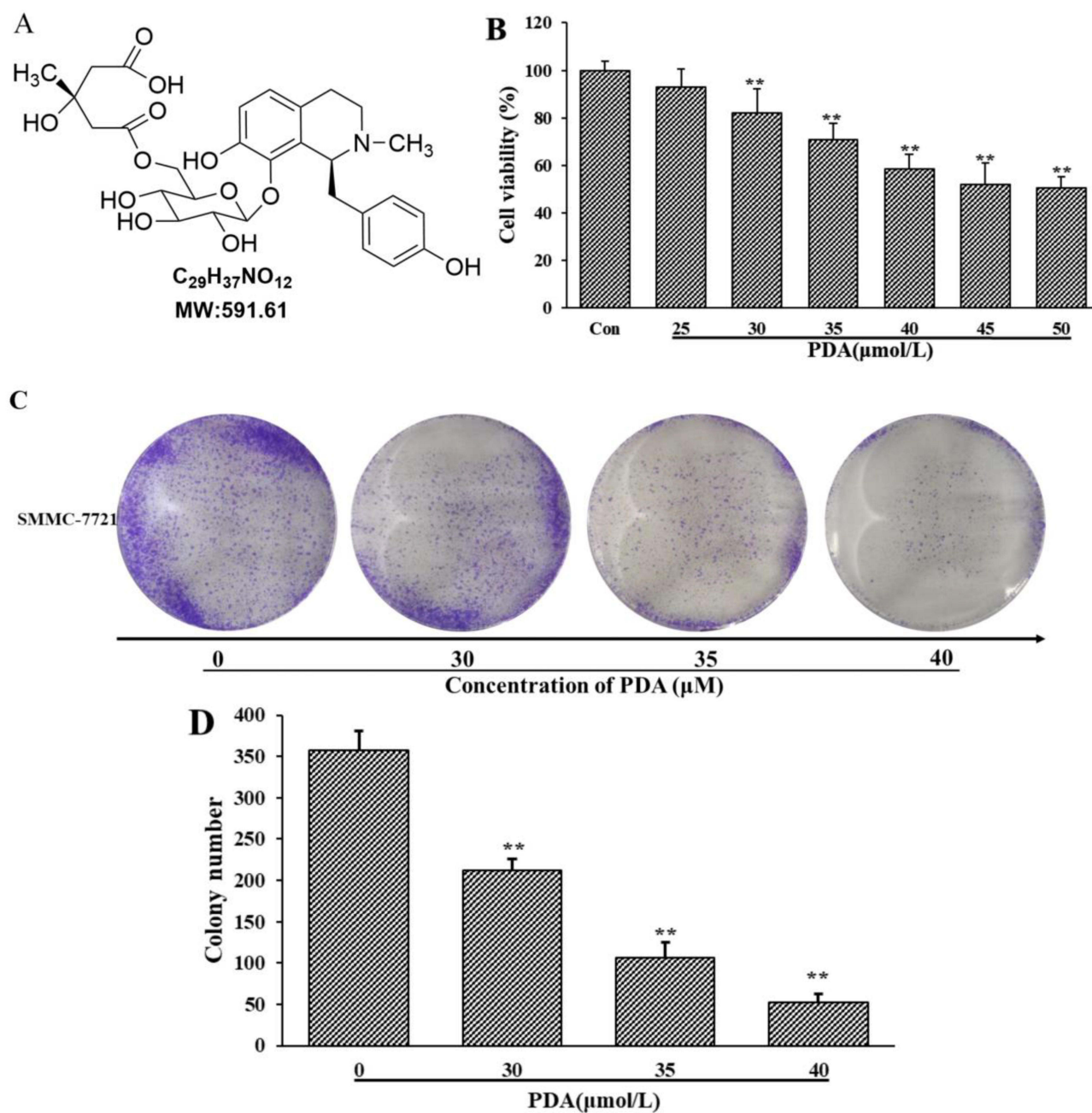


Figure 1 Anticancer effect of PDA treatment on SMMC-7721 cells. **(A)** Chemical structure of PDA. **(B)** The cytotoxicity of PDA at different concentrations (25–50 μmol/L) on SMMC-7721 cells was measured by the MTT method after 24 h treatment. **(C)** Formed colonies were stained with crystal violet. **(D)** Formed colonies were counted by using ImageJ software. The data from three independent experiments were represented as mean ± SD (n = 6). **p < 0.01 indicating statistical differences compared with the control group.

Metabolomics Analysis

Metabolomics techniques have been widely used in the discovery of candidate biomarkers for cancer staging, prognosis and treatment selection. Small-molecule metabolites in metabolic profiles are influenced by drugs or pathological processes and can provide insights into the metabolic consequences of liver disease and represent attractive candidates to understand HCC phenotypes. To this end, we have performed metabolic profiling after PDA treatment. As shown in Table 1, 696 metabolites were detected in the SMMC-7721 cell samples and were grouped into 12 known classes, but the majority of which were lipids and derivatives, amino acid and derivatives, organic acid and derivatives, nucleotide and derivatives, etc.

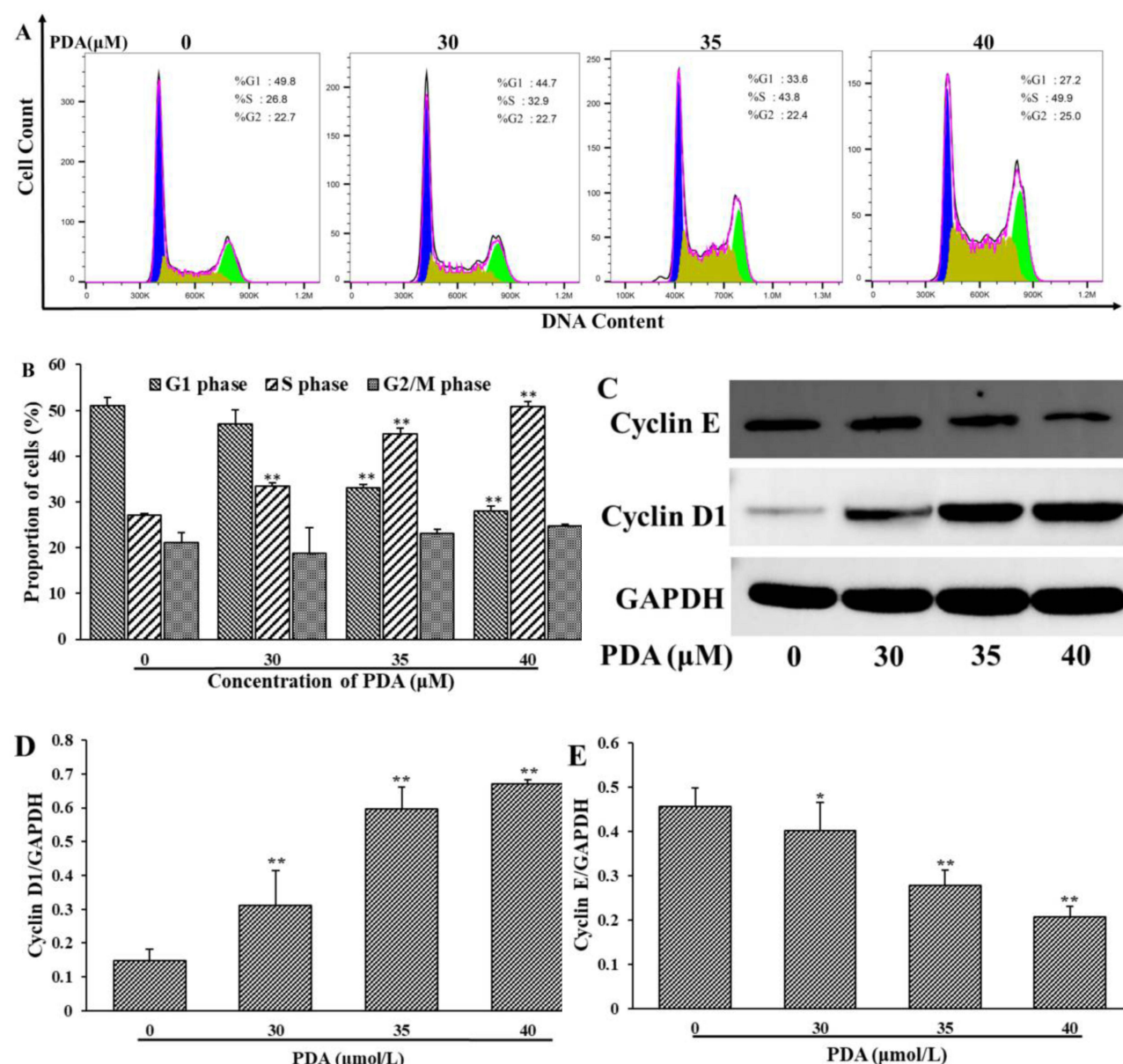


Figure 2 Effect of PDA on the cell cycle of SMMC-7721 cells. Cells were treated with PDA (0, 30, 35 and 40 μ M) for 24 h. **(A)** The proportion of cells in different phases was measured by flow cytometry. **(B)** The proportion of cells in **(A)** was statistically analyzed. **(C)** The expression of Cyclin D1 and Cyclin E was determined by Western blotting. **(D and E)** The levels of Cyclin D1 and Cyclin E were analyzed by grayscale of blots. The data of three independent experiments were demonstrated as mean \pm SD. * $p < 0.05$, ** $p < 0.01$ indicating statistical differences compared with the control group.

As shown in Figure 5A, the metabolic profile of the PDA group was significantly separated from that of the Con group according to the OPLS-DA analysis. A volcano plot was used to visually represent the differentially expressed metabolites in the PDA vs Con. This analysis screened for 144 differential metabolites in PDA vs Con (Figure 5B), among which 106 metabolites were up-regulated and 38 metabolites were down-regulated. The histogram of the top 20 differential metabolites in PDA vs Con is shown in Figure 5C (red and green markers indicate up- and down-regulation, respectively). The enrichment analysis of differential metabolites using KEGG showed that the intracellular metabolites after PDA treatment were mainly enriched in primary bile acid biosynthesis, arginine and proline metabolism, ABC transporters, notch signaling pathway and central carbon metabolism in cancer, etc. (Figure 5D). Finally, a cluster

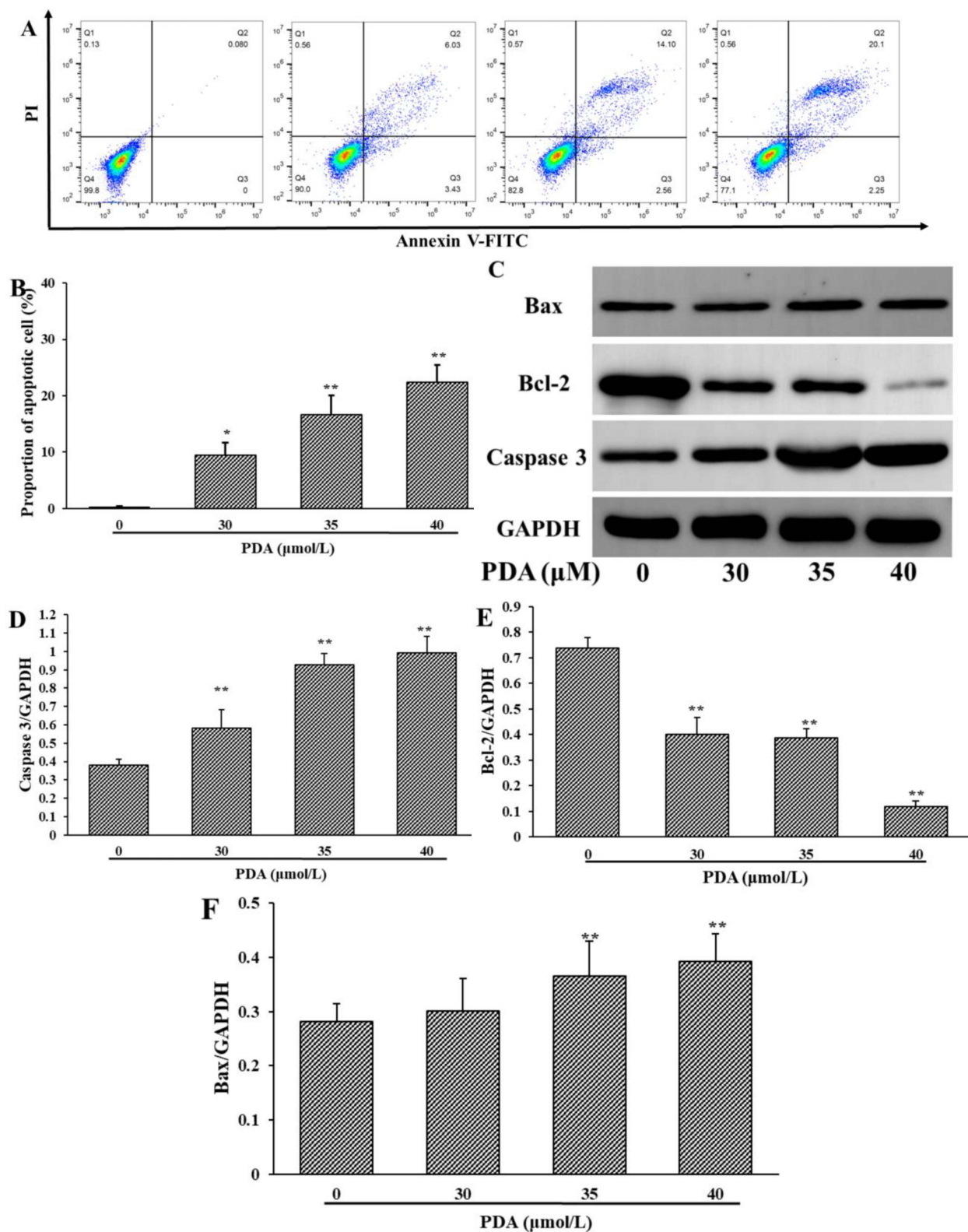


Figure 3 Effect of PDA on apoptosis level on SMMC-7721 cells. **(A)** Annexin V-FITC/PI staining presented the rate of apoptosis cells after 24 h of PDA treatment. **(B)** PDA-induced apoptosis in a dose-dependent manner. **(C–F)** Representative pictures and quantification results showed changes in the expression of Bcl-2, Bax, and cleaved-Caspase 3. The data of three independent experiments were demonstrated as mean \pm SD. * $p < 0.05$ and ** $p < 0.01$ indicating statistical differences compared with the control group.

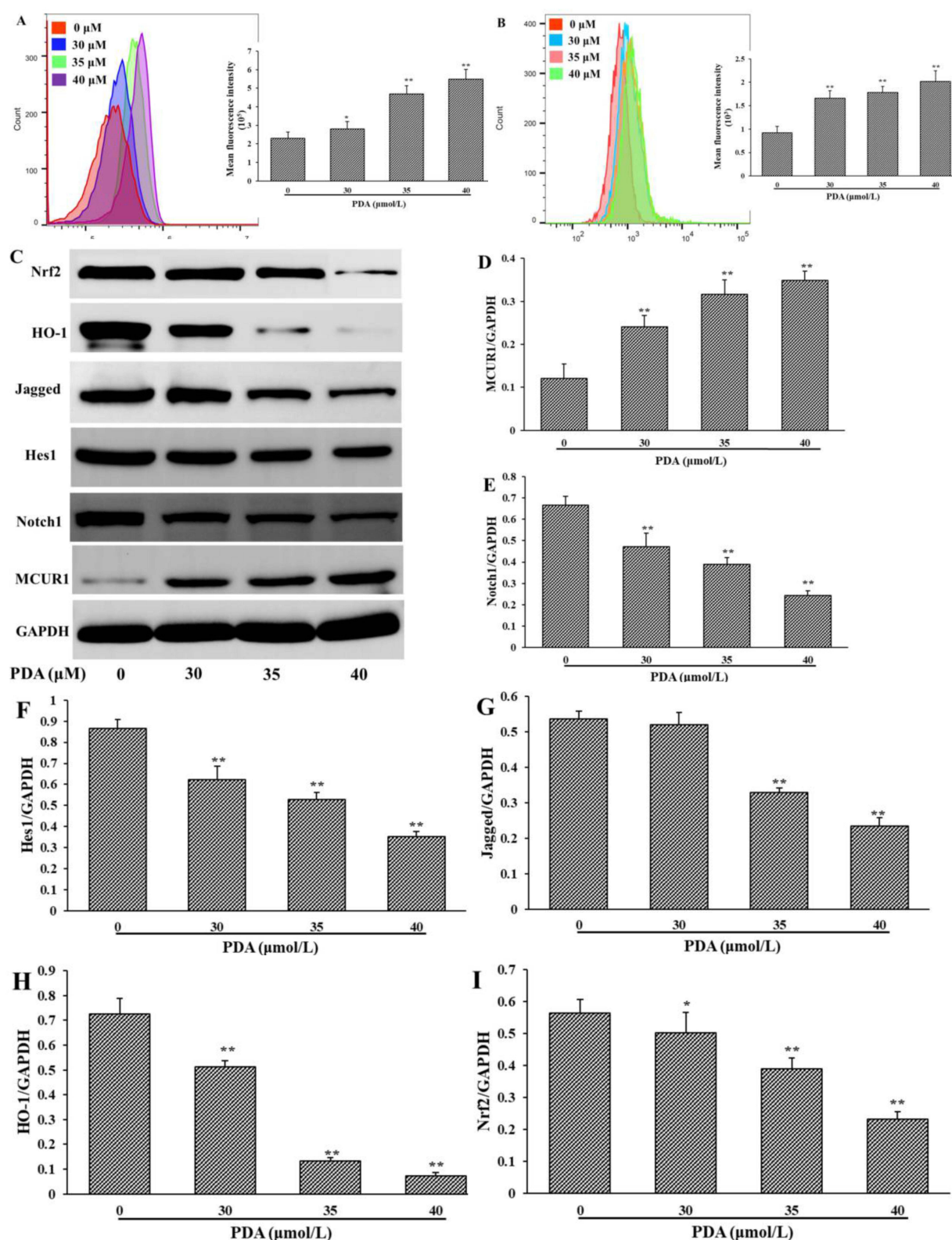


Figure 4 PDA inhibited cell proliferation via the ROS/Nrf2/Notch signaling pathway in SMMC-7721 cells. **(A)** DCFH-DA staining presented the level of ROS after 24 h of treatment. **(B)** Fluo-4 (AM) staining presented the level of Ca²⁺ after 24 h of treatment. **(C)** After 24 h of exposure to PDA, the expressions of Notch1, Jagged, Hes1, MCUR1, Nrf2 and HO-1 were analyzed by Western blotting. **(D–I)** The quantification results of Notch1, Jagged, Hes1, MCUR1, Nrf2 and HO-1 were analyzed by grayscale of blots. The data of three independent experiments were demonstrated as mean ± SD. **p* < 0.05 and ***p* < 0.01 indicating statistical differences compared with the control group.

Table I Classification of the Metabolites Detected in SMMC-7721 Cell Samples

Class	Number of Compounds
Lipid and derivative	190
Amino acid and derivative	172
Organic acid and derivative	109
Nucleotide and derivate	64
Benzene and substituted derivative	54
Heterocyclic and derivate	33
Carbohydrate	32
Others	11
Vitamins and derivative	10
Alcohol	8
Hormone	7
Bile acid	6

heatmap analysis of differential metabolites in the KEGG pathway was performed. As shown in Figure 5E, the differential metabolites in the Con group are well clustered into one group and separated from the PDA group, and most of the differential metabolites showed up-regulated PDA after treatment.

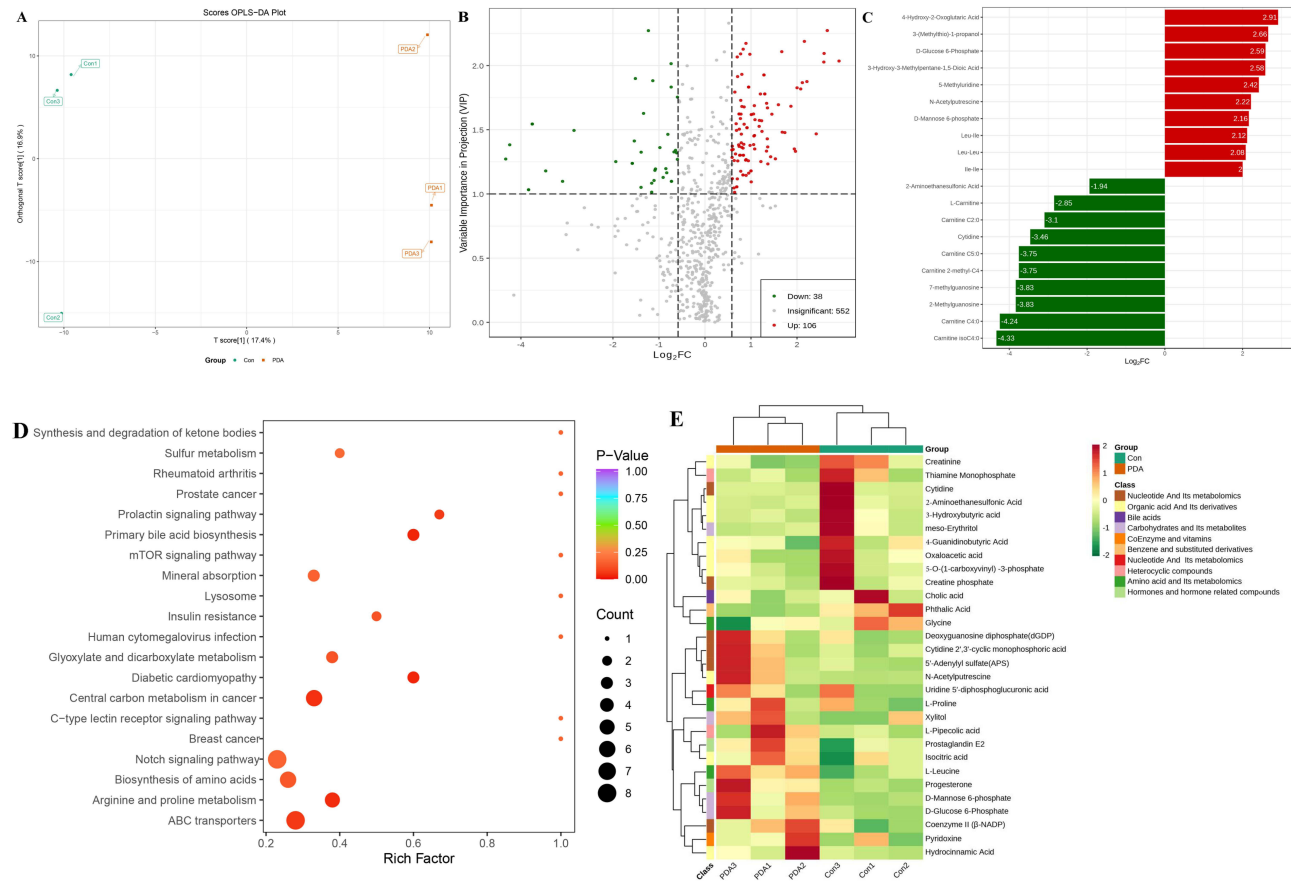


Figure 5 Score scatter plot of OPLS-DA for PDA vs Con (A). Volcano plots depicting the up-and down-regulated metabolites between pairs of samples from PDA vs Con (B). (C) The bar graphs of the top 20 differential metabolites (of them, up-regulated red-marked and down-regulated green-marked) are in PDA vs Con. (D) KEGG enrichment analysis of differential metabolites after PDA treatment. The color of the dots means the p-value (the more obvious the purple, the more significant the enrichment). The size of the dots indicates the number of enriched differential metabolites. (E) Clustering heatmap of differential metabolites in the KEGG pathway.

Discussion

Since *P. chinense* has been used for centuries in China as Chinese herbal medicine for various diseases and has an excellent therapeutic effect on inflammation diseases.¹¹ At the same time, the berberine isolated from *P. chinense* has an inhibitory effect on the proliferation of various tumor cells in addition to the treatment of inflammatory diseases. Our previous study has shown that PDA also has an anti-hepatocellular carcinoma effect. In this study, we provide substantial evidence that PDA inhibits the proliferation of SMMC-7721 cells and induced cancer apoptosis by inhibiting the ROS/Nrf2/Notch signaling pathway and significantly modulating metabolic profile.

As we all know, cell cycle progression is closely related to cell growth, and effectively controlling the proliferation of cancer cells is a key factor in the prevention and treatment of tumorigenesis.¹⁷ The DNA-binding dye PI can be used to reflect the DNA content in cells by fluorescence intensity, for which we have studied the effect of PDA on the cell cycle by flow cytometry.¹⁸ As expected, PDA arrested cell cycle on SMMC-7721 cells in the S phase, with the S phase ratio increasing from 26.8% (0 μ M) to 49.9% (40 μ M). Cyclins play a decisive role in the progression of the cell cycle, and high concentrations of cyclins bind to kinases to form complexes that are activated to help cells pass the checkpoint, and interruption of any point will hinder the entire process of cell replication.¹⁹ In mammalian cells, G1 progression is controlled by Cyclin D, which activates the cyclin-dependent kinases, followed by the activities of cyclin E–CDK2, which regulate entry into, and progression through the S phase.²⁰ Cyclin D1 and Cyclin E are essential regulators of the G1-S cell-cycle transition.²¹ It can be seen from the results that the trend of expression levels of proteins responsible for regulating the cycle is also consistent with the results of flow cytometry. PDA can significantly increase the protein expression of Cyclin D1 and reduce Cyclin E, indicating that PDA can regulate cyclins and block cell cycle to the S phase, thus inhibiting cell proliferation.

As one of the important signaling pathways for cell-to-cell contact, the Notch pathway maintains the dynamic balance between cell differentiation, proliferation and apoptosis, and plays a key role in the direction of cell differentiation.²² In recent years, more and more literature has reported that the Notch pathway plays a crucial role in liver development, repair and homeostasis, particularly closely bound up with the occurrence and development of hepatocellular carcinoma, with inappropriate activation of the Notch pathway occurring in a variety of tumors, including liver cancers.^{23,24} Numerous studies have shown that inhibiting nuclear transcription factor E2-related factor 2 (Nrf2) expression can induce tumor cell apoptosis, inhibit proliferation, metastasis and reduce chemotherapy resistance, suggesting that Nrf2 may be a potential target for tumor therapy.^{25–27} Nrf2 is present as a key regulator in the maintenance of intracellular redox homeostasis and antioxidant defense, and the activation of Nrf2 can regulate the expression of a variety of genes and proteins, thereby neutralizing ROS and restoring the REDOX balance of cells.^{28,29} Overmetabolism of cancer cells is known to lead to higher ROS levels, which can be maintained below the toxicity threshold due to the development of effective antioxidant systems.³⁰ Once ROS overproduction exceeds the toxic threshold or the antioxidant system is compromised, significant DNA damage will be caused, and cancer cells will be removed from the proliferative advantage of low or moderate ROS levels, leading to apoptosis.^{31,32} Furthermore, a study reported that Nrf2 strongly regulates Notch1 activity, reduced Nrf2 expression significantly inhibited Notch1 and heme oxygenase-1 (HO-1) expression and increased endogenous ROS levels following ionizing radiation exposure.²⁷ In the present study, the results of the Western blot showed that PDA treatment significantly inhibited Notch pathway-related proteins (notch1, Jagged, hes1) and reduced the expression of Nrf2 and HO-1. In addition, PDA treatment significantly increased intracellular ROS and Ca^{2+} levels, as well as the expression of mitochondrial Ca^{2+} uptake protein MCUR1. As a by-product of intracellular oxidative phosphorylation, an excessive increase of ROS can regulate a variety of cytokines to induce cell cycle arrest and tumor cell apoptosis.^{32,33} As a site of intracellular Ca^{2+} storage, mitochondrial function is destroyed when intracellular Ca^{2+} level overloaded occurs.³⁴ Mitochondrial uptake of calcium is a critical factor in regulating intracellular signal transduction, energy status, ROS production and cell survival.³⁵ Mitochondria uptake of Ca^{2+} depends on regulatory subunits of the mitochondrial Ca^{2+} uptake channel, such as MCUR1 (mitochondrial calcium uniporter regulator 1).³⁶ As we know, excessive intracellular ROS and dysregulation of calcium homeostasis in mitochondria can easily lead to cell apoptosis. Bcl-2, which inhibits apoptosis, and Bax, which promotes apoptosis, can bind to and inhibit each other, and their relative amounts determine whether apoptosis occurs.³⁴ Caspase-3 is the most critical apoptotic protease downstream of cascade reactions.³⁷ Flow cytometry and Western blot results indicated that PDA induced apoptosis and significantly reduce the expression of Bcl-2 and increase the expressions of Bax and Caspase 3 in SMMC-7721 cells. The above results suggested

that PDA can induce apoptosis and ultimately inhibit cell proliferation by inhibiting the ROS/Nrf2/Notch pathway. Notably, one study showed that MCUR1 knockdown significantly decreased the expression of Notch1 in the cytoplasm and its active form NICD1 in the nucleus of HCC cells, while overexpression of MCUR1 had a remarkable effect to induce the Nrf2 nuclear translocation and Notch1 activation.³⁸ As for the inconsistencies Inactivation of the downstream pathway due to MCUR1 elevation reported in the literature, it is speculated that it may be due to cell line selection. In addition, as described in their manuscript, Snail, the zinc finger protein that is a key transcriptional regulator of EMT, Snail knockdown significantly inhibited the MCUR1-induced EMT of HCC cells, and MCUR1 overexpression promoted the migration and invasion of HCC cells, which could be reversed by Snail knockdown. Snail may also be the reason for this difference, and the expression of Snail in the SMMC-7721 cell line will be further studied in subsequent experiments.

Abnormal lipid metabolism and inflammation will affect the occurrence and development of liver cancer.³⁹ A total of 144 differential metabolites were screened by metabolomics techniques, of which 38 were down-regulated, mainly including organic acids and acylcarnitines, and 106 were up-regulated, mainly including amino acids. Analysis of the metabolites in the Top 20 showed that 6 of the 10 metabolites down-regulated were carnitine derivatives, including l-Carnitine, Carnitine C2:0, Carnitine isoC4:0, Carnitine 2-methyl-C4, Carnitine C5:0, Carnitine C4:0. Acylcarnitine transport long-chain fatty acids from the cell membrane into the mitochondrial matrix.⁴⁰ Carnitine binds to long-chain acyl-coenzyme A and converts it to acylcarnitine, which is transported to mitochondria for subsequent β -oxidation to provide energy for cell activities.⁴¹ Carnitine deficiency blocks β -oxidation and causes lipid metabolism dysfunction and induces protein catabolism.⁴² A study showed that acylcarnitine concentrations increased with tumour growth in a transgenic mouse model of hepatitis B surface antigen mimicking HBV carriers, with and without aflatoxin-B1 treatment; this result was consistent with a pilot study using human serum from HCC patients.⁴³ Sorafenib, as an oral multi-target tyrosine kinase inhibitor, improves the median overall survival time of HCC patients and also inhibits the absorption of carnitine by downregulating the human organic cationic transporter OCTN2 located largely in the small intestinal mucosa and skeletal muscle.⁴⁴ In this study, the decreased levels of acylcarnitine metabolites (l-Carnitine, Carnitine C2:0, Carnitine isoC4:0, Carnitine 2-methyl-C4, Carnitine C5:0, Carnitine C4:0) after PDA treatment attenuate mitochondrial metabolism and blocked β -oxidation within mitochondria. It is noteworthy that PDA treatment can also significantly increase the levels of intracellular ROS and Ca^{2+} . As we all know, Mitochondria, as the main site of cellular energy metabolism and the generation of oxygen free radicals, were also considered to be a “ Ca^{2+} pool” with the ability to absorb a large amount of Ca^{2+} .⁴⁵ Ca^{2+} is not only an important messenger for cell proliferation, but it is also an indispensable signal for cell death. Ca^{2+} participates in and plays a crucial role in the energy metabolism, physiology, and pathology of mitochondria. Studies have shown that increased Ca^{2+} concentration in cells is transmitted into mitochondria and activates several key enzymes in the tricarboxylic acid cycle (TAC), such as pyruvate dehydrogenase, isocitrate dehydrogenase, and ketoglutarate dehydrogenase, increasing oxidative phosphorylation levels and stimulating ATP production to ultimately energy metabolism.⁴⁶ Oxidative phosphorylation in mitochondria is the main source of the production of ROS. Meanwhile, mitochondria are very sensitive targets of ROS, with significant destructive effects. Under moderate stress, the increased Ca^{2+} and ROS could enhance the corresponding signaling pathway for adapting to the elevated requirement of ATP, proliferation, and autophagy. However, once Ca^{2+} and ROS accumulation exceed the threshold, death-related events, such as apoptosis and strong autophagy. Abnormally elevated ROS and Ca^{2+} overload lead to the continuous opening of mitochondrial permeability transition pore, which results in the change of mitochondria transmembrane potential, the release of cytochrome c and the activation of caspase-3 for apoptosis.⁴⁷ These results indicated that PDA caused dysregulation of intracellular calcium homeostasis and increased ROS impair mitochondrial function, which is consistent with decreased β oxidation caused by decreased acylcarnitine metabolites.

Moreover, the Notch pathway, as one of the significantly enriched pathways by KEGG, has also been found in the metabolomics experiment, which further confirmed PDA can induce apoptosis by inhibiting ROS/Nrf2/Notch pathway. Study showed that dysregulation of Notch signaling in the liver is associated with impaired lipid metabolism, inflammation and fibrosis.²³ It was reported that lingonberry supplementation attenuated hepatic Notch1 signaling and decreased intracellular triglyceride accumulation, and thus improving lipid profile by improving the expression of the genes involved in hepatic fatty acid metabolism.⁴⁸ A study suggests that curcumin treatment can and attenuate hepatosteatosis and decrease cholesterol, triglyceride and low-density lipoprotein levels in serum by suppressing the hepatic Notch-1

pathway.⁴⁹ As expected, PDA can significantly inhibit the activation of the Notch signaling pathway in SMMC-7721 cells while reducing the level of intracellular acylcarnitine, which the inhibition of PDA on the abnormally activated Notch pathway may also affect the metabolism of intracellular acylcarnitine metabolites.

In recent years, study⁵⁰ found that the metabolites of bile acids in HCC patients were significantly different from those in healthy people, and the abnormal rise of some bile acids was believed to be closely related to the occurrence of HCC. Xie et al⁵¹ showed that the levels of taurocholic acid, glycine cholic acid, taurocholic acid, deoxycholic acid and taurocholic acid were significantly elevated in the liver of a high-fat diet-induced HCC mouse model compared to the healthy control group. The above elevated bile acid levels have been confirmed in many studies to be associated with the development and progression of HCC: for example, excessive TCA and DCA have been confirmed to induce the up-regulated expression of cancer-related inflammatory genes.⁵² Long-term exposure of hepatocytes to excess bile acids leads to sustained DNA damage, apoptosis and inflammation of hepatocytes, thus increasing the risk of inducing HCC.⁵³ Notably, PDA treatment not only inhibited the proliferation of SMMC-7721 cells but also significantly reduced the level of intracellular cholic acid and noncholic acid (Figure 5E) and the other two metabolites in the primary bile acid biosynthesis pathway: glycine, 2-aminoethanesulfonic acid (taurine) in the study. In addition, a previous study has shown that PDA possesses an excellent inhibitory effect on inflammation in vitro, and can effectively reduce nitric oxide, tumor necrosis factor- α , interleukin-1 β , and interleukin-6 pro-inflammatory mediators.¹⁰ Therefore, we speculate that the anti-inflammatory effect of PDA may be closely related to its ability to reduce the level of intracellular bile acid-related metabolites. Study⁵⁴ found that the level of total bile acids in the organ showed abnormal changes in the pathological state of the liver, and some bile acid changes may affect the activity of certain bile acid receptors, which in turn could affect the development and progression of HCC through immune inflammation or apoptosis. Farnesol X receptor, G protein-coupled receptor 1, pregnane X receptor, etc, have been confirmed to affect the development of HCC in a variety of ways. FXR can reduce the production of ROS by reducing the level of intrahepatic bile acids,⁵⁵ but in this study, PDA can significantly reduce the level of bile acid-related metabolites and increase the level of intracellular ROS. Therefore, it is speculated that PDA may inhibit the process of HCC by regulating the metabolism of bile acids.

Conclusion

In conclusion, the present study proved that hepatocellular carcinoma SMMC-7721 cells treated with PDA showed inhibition of cell proliferation and occurrence of apoptosis in vitro. It may play an anti-liver cancer effect by inhibiting the ROS/Nrf2/Notch pathway and regulating the level of intracellular acylcarnitine and bile acid-related metabolites. This study would help to deepen specific insights into the anti-hepatoma mechanisms of PDA and facilitate the clinical application of PDA as a potential therapeutic agent for hepatocellular carcinoma in the future.

Acknowledgments

We gratefully acknowledge funding supported by the Henan Provincial High-Level Talents International Training funding project (2021-72) and the Zhongjing Talent Backbone Project of Henan University of Chinese Medicine (00104311-2019-14).

Disclosure

The authors report no conflicts of interest in this work.

References

1. Caldwell S, Park SH. The epidemiology of hepatocellular cancer: from the perspectives of public health problem to tumor biology. *J Gastroenterol.* 2009;44:96–101. doi:10.1007/s00535-008-2258-6
2. Ferlay J, Soerjomataram I, Dikshit R, et al. Cancer incidence and mortality worldwide: sources, methods, and major patterns in globocan 2012. *Int J Cancer.* 2015;136:E359–86. doi:10.1002/ijc.29210
3. Sung H, Ferlay J, Siegel RL, et al. Global cancer statistics 2020: globocan estimates of incidence and mortality worldwide for 36 cancers in 185 countries. *CA Cancer J Clin.* 2021;71:209–249. doi:10.3322/caac.21660
4. Giannelli G, Koudelkova P, Dituri F, et al. Role of epithelial to mesenchymal transition in hepatocellular carcinoma. *J Hepatol.* 2016;65:798–808. doi:10.1016/j.jhep.2016.05.007

5. Bray F, Ferlay J, Soerjomataram I, et al. Global cancer statistics 2018: globocan estimates of incidence and mortality worldwide for 36 cancers in 185 countries. *CA Cancer J Clin*. 2018;68:394–424. doi:10.3322/caac.21492
6. Zhu HY, Luo H, Zhang WW, et al. Molecular mechanisms of cisplatin resistance in cervical cancer. *Drug Des Devel Ther*. 2016;10:1885–1895. doi:10.2147/DDDT.S106412
7. Meng FC, Wu ZF, Yin ZQ, et al. *Coptidis rhizoma* and its main bioactive components: recent advances in chemical investigation, quality evaluation and pharmacological activity. *Chinese Med*. 2018;13:13. doi:10.1186/s13020-018-0171-3
8. Chakraborty B, Mukerjee N, Maitra S, et al. Therapeutic potential of different natural products for the treatment of Alzheimer's Disease. *Oxid Med Cell Longev*. 2022;22:6873874.
9. Si Y, Wei W, Chen X, et al. A comprehensive study on the relieving effect of *Lilium brownii* on the intestinal flora and metabolic disorder in p-chlorophenylalanine induced insomnia rats. *Pharm Biol*. 2022;60:131–143. doi:10.1080/13880209.2021.2019283
10. Si Y, Li X, Guo T, et al. Isolation and characterization of phellodendronoside A, a new isoquinoline alkaloid glycoside with anti-inflammatory activity from *Phellodendron chinense* Schneid. *Fitoterapia*. 2021;154:105021. doi:10.1016/j.fitote.2021.105021
11. Chen ML, Xian YF, Ip SP, et al. Chemical and biological differentiation of cortex *Phellodendri chinensis* and cortex *Phellodendri amurensis*. *Planta Med*. 2010;76:1530–1535. doi:10.1055/s-0030-1249774
12. Liu D, Meng X, Wu D, et al. A natural isoquinoline alkaloid with antitumor activity: studies of the biological activities of berberine. *Front Pharmacol*. 2019;10:9. doi:10.3389/fphar.2019.00009
13. Xu Z, Feng W, Shen Q, et al. *Rhizoma coptidis* and berberine as a natural drug to combat aging and aging-related diseases via anti-oxidation and AMPK activation. *Aging Dis*. 2017;8:760–777. doi:10.14336/AD.2016.0620
14. Newman DJ, Cragg GM. Natural products as sources of new drugs from 1981 to 2014. *J Nat Prod*. 2016;79:629–661. doi:10.1021/acs.jnatprod.5b01055
15. Shang XF, Yang CJ, Morris-Natschke SL, et al. Biologically active isoquinoline alkaloids covering 2014–2018. *Med Res Rev*. 2020;40:2212–2289. doi:10.1002/med.21703
16. He D, Ma Z, Xue K, et al. Juxtamembrane 2 mimic peptide competitively inhibits mitochondrial trafficking and activates ROS-mediated apoptosis pathway to exert anti-tumor effects. *Cell Death Dis*. 2022;13:264. doi:10.1038/s41419-022-04639-6
17. Adjei AA. Blocking oncogenic Ras signaling for cancer therapy. *Jnci J Natl Cancer I*. 2001;93:1062–1074. doi:10.1093/jnci/93.14.1062
18. Chen S, Cheng AC, Wang MS, et al. Detection of apoptosis induced by new type gosling viral enteritis virus *in vitro* through fluorescein Annexin V-FITC/PI double labeling. *World J Gastroenterol*. 2008;14:2174–2178. doi:10.3748/wjg.14.2174
19. O'Connor MJ, Thakar T, Nicolae CM, et al. PARP14 regulates cyclin D1 expression to promote cell-cycle progression. *Oncogene*. 2021;40:4872–4883. doi:10.1038/s41388-021-01881-8
20. Welcker M, Clurman B. Cell cycle: how cyclin E got its groove back. *Curr Biol*. 2005;5:R810–2. doi:10.1016/j.cub.2005.09.018
21. Narasimha AM, Kaulich M, Shapiro GS, et al. Cyclin D activates the Rb tumor suppressor by mono-phosphorylation. *Elife*. 2014;2014:3.
22. Qi R, An H, Yu Y, et al. Notch1 signaling inhibits growth of human hepatocellular carcinoma through induction of cell cycle arrest and apoptosis. *Cancer Res*. 2003;63:8323–8329.
23. Geisler F, Strazzabosco M. Emerging roles of Notch signaling in liver disease. *Hepatology*. 2015;61:382–392. doi:10.1002/hep.27268
24. Zong Y, Panikkar A, Xu J, et al. Notch signaling controls liver development by regulating biliary differentiation. *Development*. 2009;136:1727–1739. doi:10.1242/dev.029140
25. Sajadimajid S, Khazaei M. Oxidative stress and cancer: the role of Nrf2. *Curr Cancer Drug Targets*. 2018;18:538–557. doi:10.2174/1568009617666171002144228
26. Zhang D, Hou Z, Aldrich KE, et al. A novel Nrf2 pathway inhibitor sensitizes keap1-mutant lung cancer cells to chemotherapy. *Mol Cancer Ther*. 2021;20:1692–1701. doi:10.1158/1535-7163.MCT-21-0210
27. Zhao Q, Mao A, Yan J, et al. Downregulation of Nrf2 promotes radiation-induced apoptosis through Nrf2 mediated Notch signaling in non-small cell lung cancer cells. *Int J Oncol*. 2016;48:765–773. doi:10.3892/ijo.2015.3301
28. de Oliveira MR, Brasil FB, Andrade CMB. Naringenin attenuates H₂O₂-induced mitochondrial dysfunction by an Nrf2-dependent mechanism in SH-SY5Y cells. *Neurochem Res*. 2017;42:3341–3350. doi:10.1007/s11064-017-2376-8
29. Xue DF, Zhou XM, Qiu JX. Emerging role of NRF2 in ROS-mediated tumor chemoresistance. *Biomed Pharmacother*. 2020;131:110676. doi:10.1016/j.biopha.2020.110676
30. Trachootham D, Alexandre J, Huang P. Targeting cancer cells by ROS-mediated mechanisms: a radical therapeutic approach. *Nat Rev Drug Discov*. 2009;8:579–591. doi:10.1038/nrd2803
31. Castaldo SA, Freitas JR, Concinha NV, et al. The tumorigenic roles of the cellular REDOX regulatory systems. *Oxid Med Cell Longev*. 2016;2016:8413032. doi:10.1155/2016/8413032
32. Sosa V, Moline T, Somoza R, et al. Oxidative stress and cancer: an overview. *Ageing Res Rev*. 2013;12:376–390. doi:10.1016/j.arr.2012.10.004
33. Moloney JN, Cotter TG. ROS signalling in the biology of cancer. *Semin Cell Dev Bio*. 2018;80:50–64.
34. Dong YJ, Gao WJ. The role of bcl-2, bax, and caspase-3 in apoptosis and its relationship. *Chin J Gerontol*. 2012;32:4828–4830.
35. Wallace DC. Mitochondria and cancer. *Nat Rev Cancer*. 2012;12:685–698. doi:10.1038/nrc3365
36. Mallilankaraman K, Cardenas C, Doonan PJ, et al. MCUR1 is an essential component of mitochondrial Ca²⁺ uptake that regulates cellular metabolism. *Nat Cell Biol*. 2012;14:1336–1343. doi:10.1038/ncb2622
37. Tan KO, Fu NY, Sukumaran SK, et al. MAP-1 is a mitochondrial effector of Bax. *Proc Natl Acad Sci USA*. 2005;102:14623–14628. doi:10.1073/pnas.0503524102
38. Jin M, Wang J, Ji X, et al. MCUR1 facilitates epithelial-mesenchymal transition and metastasis via the mitochondrial calcium dependent ROS/Nrf2/Notch pathway in hepatocellular carcinoma. *J Exp Clin Cancer Res*. 2019;38:136. doi:10.1186/s13046-019-1135-x
39. Pope ED, Kimbrough EO, Vemireddy LP, et al. Aberrant lipid metabolism as a therapeutic target in liver cancer. *Expert Opin Ther Targets*. 2019;23:473–483. doi:10.1080/14728222.2019.1615883
40. Qu Q, Zeng F, Liu X, et al. Fatty acid oxidation and carnitine palmitoyltransferase I: emerging therapeutic targets in cancer. *Cell Death Dis*. 2016;7:e2226. doi:10.1038/cddis.2016.132
41. Tarasenko TN, Cusmano-Ozog K, McGuire PJ. Tissue acylcarnitine status in a mouse model of mitochondrial beta-oxidation deficiency during metabolic decompensation due to influenza virus infection. *Mol Genet Metab*. 2018;125:144–152. doi:10.1016/j.ymgme.2018.06.012

42. Magoulas PL, El-Hattab AW. Systemic primary carnitine deficiency: an overview of clinical manifestations, diagnosis, and management. *Orphanet J Rare Dis*. 2012;7:68. doi:10.1186/1750-1172-7-68
43. Yaligar J, Teoh WW, Othman R, et al. Longitudinal metabolic imaging of hepatocellular carcinoma in transgenic mouse models identifies acylcarnitine as a potential biomarker for early detection. *Sci Rep*. 2016;6:20299. doi:10.1038/srep20299
44. Amanuma M, Nagai H, Igarashi Y. Sorafenib might induce sarcopenia in patients with hepatocellular carcinoma by inhibiting carnitine absorption. *Anticancer Res*. 2020;40:4173–4182. doi:10.21873/anticancer.14417
45. Denton R. Regulation of mitochondrial dehydrogenases by calcium ions. *Biochim Biophys Acta*. 2009;1787:1309–1316. doi:10.1016/j.bbabi.2009.01.005
46. Zhang L, Qi J, Zhang X, et al. The regulatory roles of mitochondrial calcium and the mitochondrial calcium uniporter in tumor cells. *Int J Mol Sci*. 2022;23:6667. doi:10.3390/ijms23126667
47. Zhou Y, Jing S, Liu S, et al. Double-activation of mitochondrial permeability transition pore opening via calcium overload and reactive oxygen species for cancer therapy. *J Nanobiotechnology*. 2022;20:188. doi:10.1186/s12951-022-01392-y
48. Madduma Hewage S, Au-Yeung KKW, Prashar S, et al. Lingonberry improves hepatic lipid metabolism by targeting Notch1 signaling. *Antioxidants*. 2022;11:472. doi:10.3390/antiox11030472
49. Zhao NJ, Liao MJ, Wu JJ, et al. Curcumin suppresses Notch-1 signaling: improvements in fatty liver and insulin resistance in rats. *Mol Med Rep*. 2018;17:819–826. doi:10.3892/mmr.2017.7980
50. Gao L, Lv G, Li R, et al. Glycochenodeoxycholate promotes hepatocellular carcinoma invasion and migration by AMPK/mTOR dependent autophagy activation. *Cancer Lett*. 2019;454:215–223. doi:10.1016/j.canlet.2019.04.009
51. Xie G, Wang X, Huang F, et al. Dysregulated hepatic bile acids collaboratively promote liver carcinogenesis. *Int J Cancer*. 2016;139:1764–1775. doi:10.1002/ijc.30219
52. Allen K, Jaeschke H, Copple BL. Bile acids induce inflammatory genes in hepatocytes: a novel mechanism of inflammation during obstructive cholestasis. *Am J Pathol*. 2011;178:175–186. doi:10.1016/j.ajpath.2010.11.026
53. Beuers U, Bilzer M, Chittattu A, et al. Tauroursodeoxycholic acid inserts the apical conjugate export pump, Mrp2, into canalicular membranes and stimulates organic anion secretion by protein kinase C-dependent mechanisms in cholestatic rat liver. *Hepatology*. 2001;33:1206–1216. doi:10.1053/jhep.2001.24034
54. Chiang J, Ferrell JM. Bile acids as metabolic regulators and nutrient sensors. *Annu Rev Nutr*. 2019;39:175–200.
55. Nomoto M, Miyata M, Yin S, et al. Bile acid-induced elevated oxidative stress in the absence of farnesoid X receptor. *Biol Pharm Bull*. 2009;32:172–178.

Publish your work in this journal

The Journal of Hepatocellular Carcinoma is an international, peer-reviewed, open access journal that offers a platform for the dissemination and study of clinical, translational and basic research findings in this rapidly developing field. Development in areas including, but not limited to, epidemiology, vaccination, hepatitis therapy, pathology and molecular tumor classification and prognostication are all considered for publication. The manuscript management system is completely online and includes a very quick and fair peer-review system, which is all easy to use. Visit <http://www.dovepress.com/testimonials.php> to read real quotes from published authors.

Submit your manuscript here: <https://www.dovepress.com/journal-of-hepatocellular-carcinoma-journal>